Electronic Supplementary Information (ESI) for

Naphthalene-fused BODIPY Near-Infrared Dye as A Stable Contrast Agent for *In Vivo* Photoacoustic Imaging

Yong Ni, Ravi K. Kannadorai, Juanjuan Peng, Sidney W. -K. Yu, Young-Tae Chang, Jishan Wu**

Table of Content

1. Experimental section

1.1 General

All reagents were purchased from commercial suppliers and used as received without further purification. Anhydrous dichloromethane (DCM) was distilled from CaH_2, anhydrous THF and toluene were distilled from sodium. The ^1H NMR and ^{13}C NMR spectra were recorded in solution of $CDCl_3$ on Bruker DPX 300 or DRX 500 NMR spectrometers with tetramethylsilane (TMS) as the internal standard. The following abbreviations were used to explain the multiplicities: s = singlet, d = doublet, t = triplet, m = multiplet. MALDI-TOF mass spectra were measured on a Bruker Autoflex MALDI-TOF instrument using 1,8,9- trihydroxyanthracene as a matrix. HR-APCI mass spectra were recorded on MicrOTOF-Q II 10269 mass spectrometer. UV-vis-NIR absorption spectra were recorded on a Shimadzu UV-1700 spectrometer. The solvents used for UV-vis and fluorescence measurements are of HPLC grade. The electrochemical measurements were carried out in anhydrous DCM with 0.1 M tetrabutylammonium hexafluorophosphate (Bu_4NPF_6) as the supporting electrolyte at a scan rate of 0.05 V/s at room temperature under the protection of nitrogen.

1.2 Synthetic procedures and characterization data

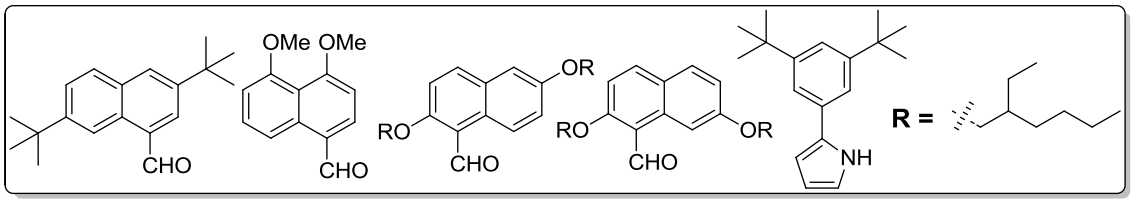

All these compounds were synthesized according to the literature procedure.[1]

General Procedure for Synthesis of BODIPY structures: To a solution of corresponding aldehyde (0.655 mmol) and pyrrole (1.64mmol, 2.5eq) in degassed anhydrous DCM (50 mL) was added four drops of TFA. The reaction mixture was stirred at room temperature for three hours under nitrogen atmosphere. Then DDQ (0.79 mmol, 141mg) was added, and the solution was stirred at room temperature for another 1 h under nitrogen atmosphere. Et_3N (3 mL, excess) and $BF_3{\cdot}OEt_2$ (4 mL, excess) were successively added. After 4 h the solvents were removed under reduced pressure, and the

residue was purified by column chromatography (silica gel, DCM: hexane = 1:6).

Compound 1:

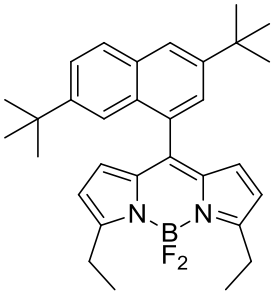

Yield 55%. ^{1}H NMR (300 MHz, $CDCl_3$): δ = 7.85 – 7.76 (m, 3H), 7.57 (m, 2H), 6.55 (d, *J* = 4.2 Hz, 2H), 6.27 (d, *J* = 4.2 Hz, 2H), 3.18 – 3.07 (m, 4H), 1.41 (s, 9H), 1.37 (t, *J* = 7.6 Hz, 6H), 1.26 (s, 9H) ppm. ^{13}C NMR (75MHz, $CDCl_3$): δ = 164.2, 149.4, 147.4, 142.8, 136.0, 132.4, 131.9, 131.5, 131.1, 128.7, 128.3, 125.8, 125.1, 121.7, 117.7, 35.6, 35.4, 31.8, 22.8, 13.4 ppm. HR-MS (MALDI-TOF): *m/z* = 486.3021 ($[M]^+$), calcd for $C_{31}H_{37}BF_2N_2$:486.3012.

Compound 2:

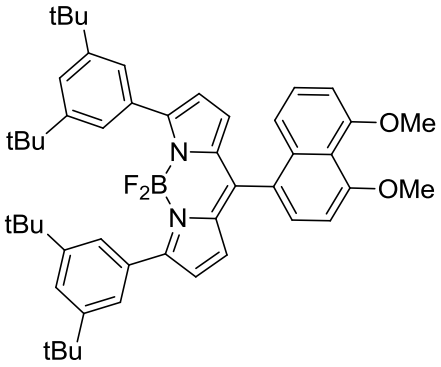

Yield 57 %. ^{1}H NMR (300 MHz, $CDCl_3$): δ = 7.72 (d, *J* = 1.7 Hz, 4H), 7.57 – 7.43 (m, 4H), 7.36 (t, *J* = 8.1 Hz, 1H), 6.93 (m, 2H), 6.61 (d, *J* = 4.2 Hz, 2H), 6.47 (d, *J* = 4.2 Hz, 2H), 4.08 (s, 3H), 4.03 (s, 3H), 1.35 (s, 36H) ppm. ^{13}C NMR (75 MHz, $CDCl_3$): δ = 159.88, 158.41, 157.14, 150.22, 142.63, 137.46, 136.66, 132.21, 130.11, 129.17, 127.17, 124.03, 123.61, 120.77, 119.61, 117.37, 106.52, 104.74, 56.52, 56.39, 34.91, 31.48 ppm. HR-MS (APCI): *m/z* = 755.4584 ($[M+H]^+$), calcd for $C_{49}H_{57}BF_2N_2O_2$: 754.4481; $C_{49}H_{58}BF_2N_2O_2$: 755.4562.

Compound 3:

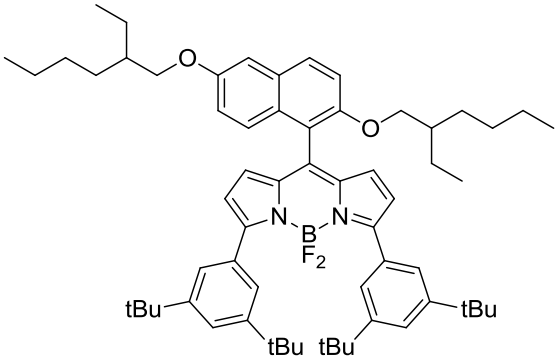

Yield 52%. ^{1}H NMR (300 MHz, $CDCl_3$) δ = 7.87 (d, *J* = 9.0 Hz, 1H), 7.75 (s, 4H), 7.65 (d, *J* = 9.1 Hz, 1H), 7.45 (s, 2H), 7.37 (d, *J* = 9.1 Hz, 1H), 7.19 – 7.10 (m, 2H), 6.54 (m, 2H), 6.46 (m, 2H), 3.96 (m, 4H), 1.53 (s, 2H), 1.36 (s, 36H), 1.27 (m, 6H), 1.19 (m, 8H), 0.97 (m, 8H), 0.79 (d, *J*=8.1, 6H) ppm. ^{13}C NMR (75 MHz, $CDCl_3$): δ = 159.61, 156.04, 153.12, 150.16, 139.55, 137.48, 132.37, 129.56, 129.38, 126.85, 123.67, 123.51, 120.50, 120.38, 117.82, 115.05, 106.35, 72.47, 70.54, 39.49, 39.43, 34.92, 31.51, 30.62, 30.30, 29.69, 29.12, 28.92, 23.96, 23.68, 23.06, 22.90, 14.09, 11.15, 11.06 ppm. HR-MS (MALDI-TOF): *m/z* = 950.6630 ($[M]^+$), calcd for $C_{63}H_{85}BF_2N_2O_2$: 950.6672.

Compound 4:

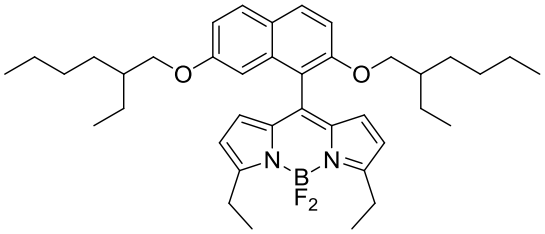

Yield 45%. ^{1}H NMR (500 MHz, $CDCl_3$): δ = 7.84 (d, *J* = 8.9 Hz, 1H), 7.70 (d, *J* = 9.0 Hz, 1H), 7.16 (d, *J* = 8.9 Hz, 1H), 7.02 (d, *J* = 9.0 Hz, 1H), 6.86 (s, 1H), 6.48 (d, *J* = 3.5 Hz, 2H), 6.23 (d, *J* = 3.6 Hz, 2H), 3.88 (d, *J* = 5.3 Hz, 2H), 3.81 – 3.73 (m, 2H), 3.18 – 3.07 (m, 4H), 1.64 (m, 1H), 1.52 (m, 1H), 1.36 (m, 8H), 1.32 – 1.22 (m, 6H), 1.13 (m, 8H), 0.87 (m, 6H), 0.81 (t, *J* = 6.6 Hz, 3H), 0.73 (t, *J* = 7.4 Hz, 3H) ppm. ^{13}C-NMR (126 MHz, $CDCl_3$): δ = 162.94, 158.18, 155.23, 139.26, 135.50, 135.40, 130.51, 129.49, 129.13, 123.83, 116.87, 116.58, 115.79, 111.19, 104.46, 71.55, 70.43, 39.35, 39.02, 30.50, 30.28, 28.96, 28.87, 23.72, 23.57, 22.94, 22.85, 22.03, 13.96, 12.66, 11.08, 10.96

ppm. HR-MS (MALDI-TOF): *m/z* = 630.4162 ($[M]^+$), calcd for $C_{39}H_{53}BF_2N_2O_2$: 630.4163.

General procedure of the oxidative cyclo-dehydrogenation reaction of the *meso*-naphthalene substituted BODIPYs: To a solution of un-fused naphthalene BODIPY precursors (0.079 mmol) in degassed anhydrous DCM (30 mL) was added a solution of $FeCl_3$ (32.5 mg, 0.198 mmol, 2.5 equal) in nitromethane (1.0 mL). The reaction mixture was carried out at room temperature until the starting materials disappeared and then quenched by addition of a saturated $NaHCO_3$ solution (5 mL). The organic layer was washed with saturated brine and dried over anhydrous Na_2SO_4. The solvent was removed under vacuum and the residue was purified by column chromatography (silica gel, DCM: hexane = 1:4). Upon treatment with $FeCl_3$, only the BODIPY precursor **4** can afford the fused-BODIPY structure in good separation yield.

Compound Na-BD:

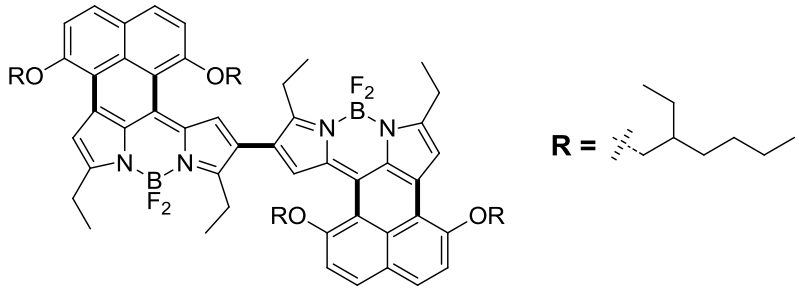

Yield 48%. ^{1}H NMR (500 MHz, $CDCl_3$): δ = 8.04 (d, *J* = 8.8 Hz, 2H), 7.91 (d, *J* = 9.0 Hz, 2H), 7.49 (s, 2H), 7.30 (m, 4H), 7.15 (s, 2H), 4.28 (d, *J* = 4.3 Hz, 4H), 3.23 (q, *J* = 7.5 Hz, 4H), 3.07 (q, *J* = 7.0 Hz, 4H), 2.01 (m, 2H), 1.68 (m, 8H), 1.46 (t, *J* = 7.5 Hz, 6H), 1.29 (m, 12H), 1.25 (s, 12H), 1.12 – 1.06 (m, 8H), 1.02 (t, *J* = 7.5 Hz, 6H), 0.92 (t, *J* = 7.1 Hz, 6H), 0.70 (m, 12H) ppm. ^{13}C NMR (126 MHz, $CDCl_3$): δ = 164.32, 161.21, 159.42, 154.57, 136.94, 134.82, 133.76, 131.41, 130.71, 130.34, 126.80, 126.30, 122.92, 122.85, 113.86, 113.76, 113.38, 110.98, 108.97, 77.28, 77.03, 76.78, 74.37, 71.92, 39.84, 38.98, 30.80, 30.21, 29.26, 28.72, 24.07, 23.57, 23.10, 22.79, 22.21, 20.93, 14.64, 14.07, 13.83, 12.91, 11.29, 10.64 ppm. HR-MS (MALDI-TOF): *m/z* = 1254.7885 ($[M]^+$), calcd for $C_{78}H_{100}B_2F_4N_4O_4$: 1254.7861.

2. Optical and electrochemical properties

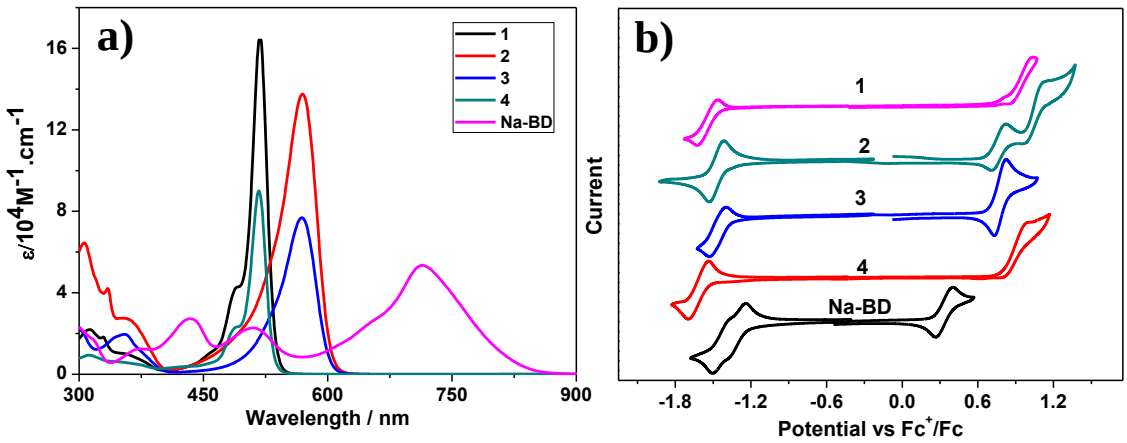

Fig. S1. Absorption spectra (a) and cyclic voltammograms (b) of compounds **1**, **2**, **3**, **4** and **Na-BD**.

Compounds	E_{ox}^{1}	E_{ox}^{2}	E_{red}^{1}	**HOMO**	**LUMO**	E_g^a	ΔE_g^{opt}
	(V)	(V)	(V)	(eV)	(eV)	(eV)	(eV)
1	0.95	-	-1.52	-5.61	-3.36	2.25	2.28
2	0.68	1.04	-1.48	-5.42	-3.40	2.02	2.03
3	0.75	1.13	-1.47	-5.46	-3.42	2.04	2.05
4	0.90	-	-1.62	-5.57	-3.29	2.28	2.30
Na-BD	0.34	-	-1.37	-5.05	-3.59	1.46	1.48

Table S1. Summary of electrochemical properties of compounds **1**, **2**, **3**, **4** and **Na-BD**. E_{ox}^{n} and E_{red}^{n} are the half-wave potentials for respective redox waves with Fc/Fc^{+} as reference. HOMO and LUMO energy levels were calculated from the onset of the first oxidation and reduction waves according to equations: HOMO = -(4.8 + E_{ox}^{onset}) and LUMO = - (4.8 + E_{red}^{onset}).[6] E_g^a Obtained from cyclic voltammograms. ΔE_g^{opt} Obtained from the low energy.

3. Photo-stability of Na-BD and ICG

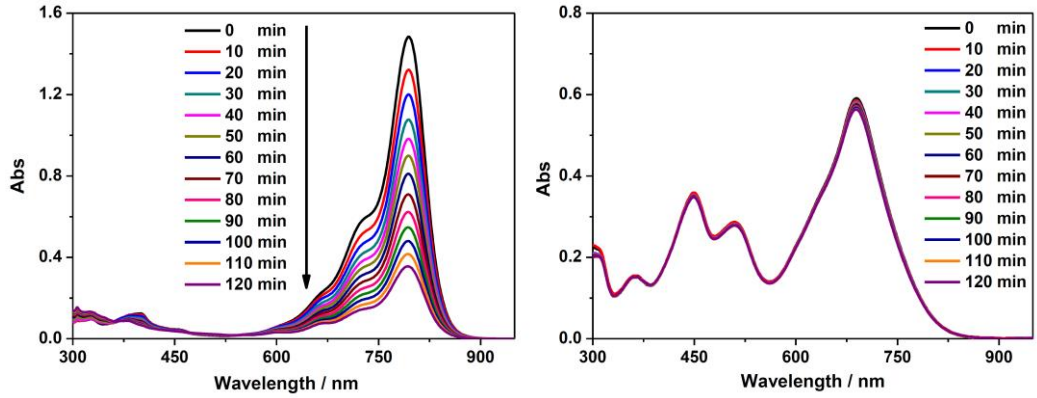

Fig. S2. Photo-stability measurement of **ICG** and **Na-BD** in solution phase. Firstly, the DMSO solution of **ICG** and **Na-BD** were kept in sealed UV-cell under 100w white light, the abs spectrum of **ICG** (left) and **Na-BD** (right) in DMSO solution after different irradiation time.

4. Methods and results of photoacoustic imaging in tissue-mimicking phantom

Statement: all experiments were performed in compliance with the relevant laws and institutional guidelines, and our institutional committee Singhealth has approved the experiments (IACUC no.: 2014/SHS/931). We did not use human subjects.

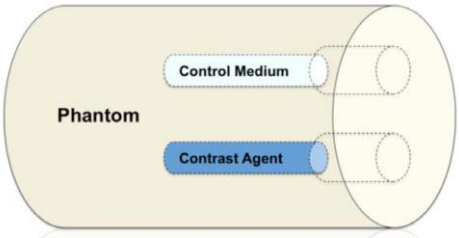

Fig. S3. Schematic tissue-mimicking phantom.

MSOT experimental parameters and protocol. All phantom imaging experiments were performed using a real-time multispectral optacoustic tomographic (MSOT) imaging system; in Vision 64 (iThera Medical GmbH, Neuherberg, Germany). The phantom provided by iThera itself is made of polyurethane, cylindrical in shape with a diameter of 2 cm, which is specially designed to mimic the shape, size and optical properties of tissue. In addition, it has 2 inner cylindrical channels, each with a diameter

of 3 mm and ~ 200 µL capacities, one for holding the control medium and the other for holding the dissolved contrast agent in the same medium, as shown in Fig. S3. Laser excitation was provided by a Q-switched Nd:YAG laser with a tunable NIR wavelength range from 680 to 980 nm with a pulse duration of 10 ns and repetition rate of 10 Hz. The sample was illuminated at different angles around the imaging plane by delivering the laser via fiber bundle divided into 10 output arms. PA signals were acquired using a 64-element concave transducer array forming an arc of 270º. Thetransducer's 5 MHz central frequency provides a transverse spatial resolution of about 150–200 µm. One transverse image slice can be acquired from each laser pulse, resulting in a frame-rate of 10 Hz. During image acquisition, the sample is translated through the transducer array by the translation stage along its axis, in order to capture the corresponding transverse image slices.

When measuring the PA activity of **Na-BD** and **ICG** in solution phase, DMSO of both dyads with concentration of 2uM, 4uM, 6uM, 8uM, 10uM was prepared, and the phantom test was then conducted from the low concentration to high concentration based on the pre-described procedures. The data was collected by scanning from 680 nm to 900 nm with an interval of 10 nm, images were reconstructed using a model-based approach[2] for offline analysis. After image reconstruction, spectral unmixing was performed to resolve individual components from different chromophores in the system. For each pixel in the image, the method fits the total measured optoacoustic spectrum to the known absorption spectra of the individual chromophores, based on least-squares linear regression.

PA signal intensity at the wavelength of absorption maximum for **Na-BD** (700 nm) and **ICG** (790 nm) at different concentrations (from 2 uM to 10 uM) was selected for comparing the PA activity of both dyads. Although the absorption maximum wavelengths of Na-BD and ICG are quite different; however, both of the wavelengths lie in the NIR region, which tends to be a biocompatible window to be used for in vivo imaging applications. Thus it is reasonable to describe the PA activity of both Na-BD and ICG by the single-wavelength PA signal intensity of both dyads. The PA signal for each contrast agent was spectrally unmixed via linear regression. This allows the

isolation of the individual contribution of the contrast agent of interest that can be plotted as a function of concentration, which in turn was used to produce a straight line of best fit based on least-squares regression, for both **Na-BD** and **ICG**. The comparison between the gradient of the plotted linear lines can give us intuitive information for the PA activity of both dyads, thereby **Na-BD** with much higher plotted-linear-gradient exhibited higher PA activity.

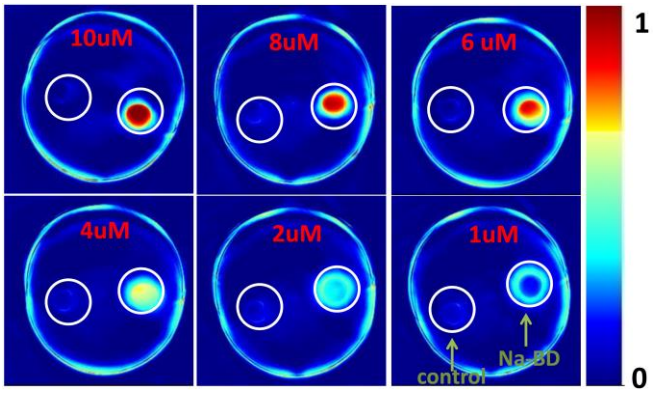

Fig. S4. Concentration dependent PA images of **Na-BD** in DMSO solution from phantom test.

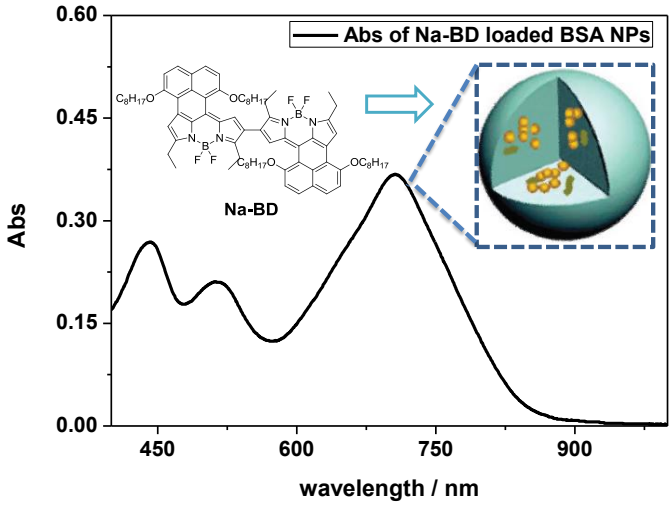

Fig. S5. Absorption spectrum of **Na-BD** loaded BSA NPs in aqueous solution that was used for photoacoustic phantom test. (According to the calibration curve of **Na-BD**, the concentration of the Na-BD loaded BSA NPs was estimated as **7.723 ug·mL^{-1}**. For the concentration dependent photoacoustic test, the other concentration of the NPs was diluted from this solution, by 2, 4, 8, 16 times respectively.)

5. Fabrication and characterization of Na-BD loaded BSA NPs

Fabrication of Na-BD loaded BSA NPs: The NPs were prepared with varied feeding ratios ranging from 0.25 to 2.5 wt%, defined as the ratio of the weight of the **Na-BD** to that of the BSA in the feed mixture. In brief, 13 mg of BSA were dissolved in 5 mL of Milli-Q water. Subsequently, 2 mL of THF containing a predetermined amount of **Na-BD** were added dropwise into the aqueous solution of BSA under sonication at room temperature, using a microtip probe sonicator with an 18 W output (XL2000, Misonix Incorp., USA), leading to the formation of the **Na-BD** loaded BSA NPs (the mixture would be somehow heated due to sonication). Until the mixture cooled down to room temperature, a small amount (100 µL) of glutaraldehyde solution (2.5 %) was then added to cross-link the NPs at RT for 4 h. The THF was removed by rotary evaporation under vacuum. The cross-linked **Na-BD** loaded BSA-NP suspension was filtered through a 0.45 µm microfilter and was then washed with Milli-Q water. The amounts of the dyes successfully encapsulated into the BSA NPs were determined from the absorption spectra with reference to a calibration curve established from dimethyl sulfoxide (DMSO) solutions of **Na-BD**. The EE is defined as the ratio of the amount of the **Na-BD** dye loaded in the NPs to the total amount of the **Na-BD** in the feed mixture.

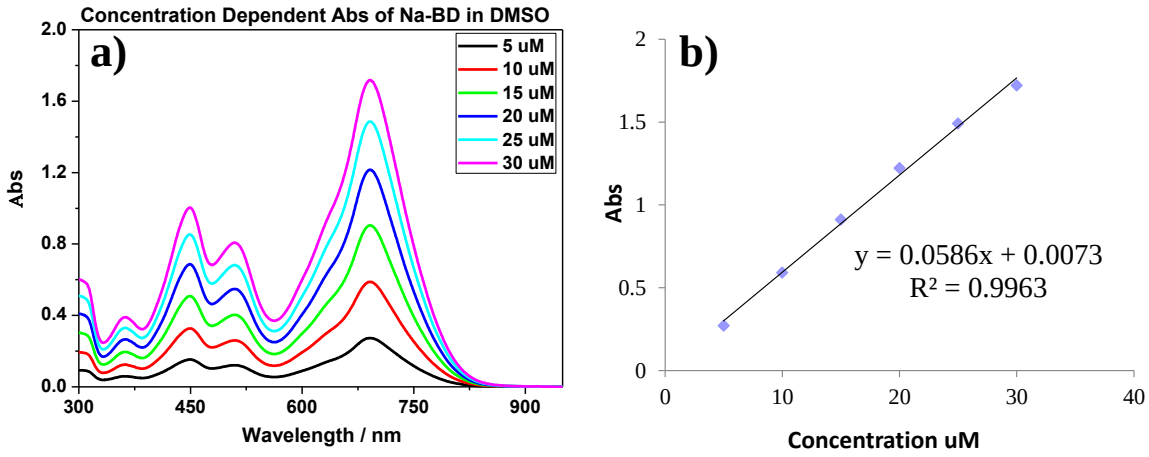

Fig. S6. Cocentration dependent absorption spectrum a) of **Na-BD** in DMSO solution and the calibration curve b).

Na-BD feeding ratio[a)] [wt %]	Na-BD loading ratio[b)] [wt %]	Encapsulation efficiency [EE %]	Size[c)] [nm] (PDI)[d)]

0	0	0	51.3(0.659)
0.25	0.25	100	133.9 (0.395)
0.5	0.48	95.5	133.0 (0.270)
1.0	0.76	75.7	145.6 (0.267)
2.5	1.58	63.2	141.2 (0.334)
5.0	2.56	51.2	171.6 (0.383)

Table S2. Characteristics of the BSA NPs loaded with **Na-BD** at different feeding ratio. [a)]The ratio of the weight of **Na-BD** to that of BSA in feed mixture; [b)]The ratio of the weight of the loaded **Na-BD** to that of the BSA matrix in the NPs; [c)]Average diameter of the NPs measured by laser light scattering (LLS); [d)]Polydispersity index (PDI).

6. Methods and results of photoacoustic imaging *in vivo*

All *in vivo* mouse imaging experiments were performed using a real-time multispectral optacoustic tomographic (MSOT) imaging system; in Vision 64 (iThera Medical GmbH, Neuherberg, Germany), the MSOT experimental parameters and protocol procedure were the same as the imaging test in phantom (see S4). For *in vivo* imaging, ultrasound gel was applied on the mouse skin surface and measurements were recorded in temperature-controlled water for good acoustic coupling. An animal holder with a thin polyethylene membrane was used to prevent direct contact between the mouse and the water. The animal stage allows in-plane object translation over 150 mm with 0.1 mm grid size for data acquisition. Prior to placing the animal in the scanning chamber the animal is knocked down in an isoflurane chamber. During the scan period the animal is placed in a belly down position and anesthetized by continuously maintaining the isoflurane at 1.5 – 2 % at an oxygen flow rate of 0.8 – 1.5 mL/min. The multispectral tomographic images were obtained by averaging 5 sample sets per wavelength. For the acquiring photoacoustic signals the MSOT system wavelength range was set to 700 - 900 nm with an interval of 10 nm for each axial slice, and recorded the averaged photoacoustic signals from 5 frames per wavelength at each step. Signals obtained were then processed to reconstruct the anatomical and functional (multispectral) tomographic images using the integrated *ViewMSOT* software.

For the **Na-BD** loaded BSA NPs solution that would be injected to the Hep-G2-tumor mice, it was firstly diluted by 10 times before measuring the absorption spectrum (since

the solution was too concentrated, and the absorption would be saturated), the absorption spectrum was then measured, as shown in Fig. S6, the concentration of the **Na-BD** loaded BSA NPs injected to Hep-G2-tumor mice was estimated to be **143.8 μg/mL** referring to the calibration curve.

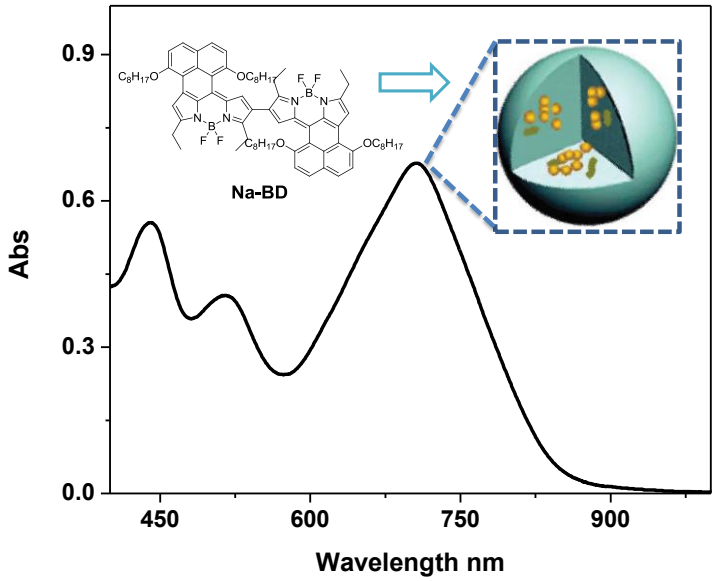

Fig. S7. Absorption spectrum of **Na-BD** loaded BSA NPs solution injected to Hep-G2-tumor mice (diluted by 10 times).

7. Cell Culture and preparation of Hep-G2-tumor mice model

Hep-G2 liver cancer cells were cultured in Dulbecco's Modified Eagle's Medium (DMEM) containing 10% fetal bovine serum (FBS) and 1% penicillin streptomycin at 37°C in an incubator containing 5% CO2. When 80-90% confluent, cells were used for subcutaneous innoculation. Xenograft models were established by subcutaneous injection of 5×106 cells on the right flank of a Balb/C nude mouse. The mice was continuously monitored for the tumor growth and was used for further experiments when the tumor volume reached a size of 1000 mm^3.

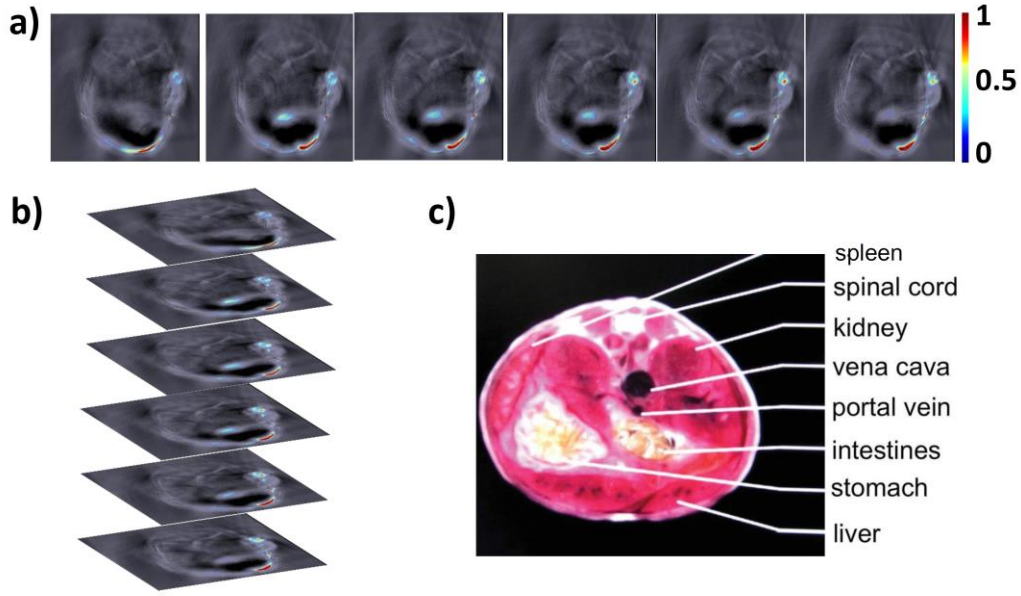

Fig. S8. Single-wavelength PAI of a Hep-G2-tumor bearing mice anatomy at 700 nm. a) Individual anatomy sections recorded after 48 hours post-intravenous injection of Na-BD loaded BSA NPs, images were acquired at a constant distance of 1 mm between each axial plane of analysis that covered the entire tumor region; b) three-dimensional rendering of the scanning area before injection and at 48 hours post injection; c) Schematic section of living mice.

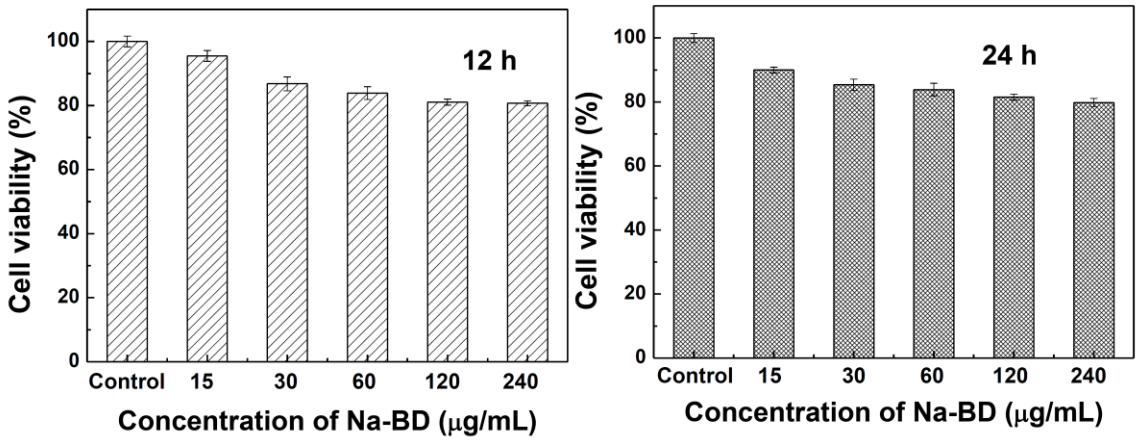

Figure S9. Cell viability values (%) estimated by MTT proliferation tests versus incubation concentrations of **Na-BD** loaded BSA NPs. HeLa cells were cultured in the presence of **Na-BD** loaded BSA NPs at 37 ^{o}C for 12h and 24 h, respectively.

8. References

[1]. a) U. Fahnenstich, K. H. Koch, K. MÜllen, *Makromol. Chem., Rapid Commun.*, **1989**, *10*, 563–569; b) A. OhIemachera, R. Schenka, H. P. Weitzel, N. ZjutyuIkov, M. Tasseva, K. MÜllen, *Makromol. Chem.*, **1992**, *193*, 81-93; c) U. Boas, J. B. Christensen, K. J. Jensen, *J. Comb. Chem.* **2004,** *6*, 497-503.

[2]. A. Rosenthal, D. Razansky, V. Ntziachristos, *IEEE Trans. Med. Imag.* **2010**, 29, 1275.

9. Appendix: ^{1}H, ^{13}C NMR, HR mass spectra of new compounds

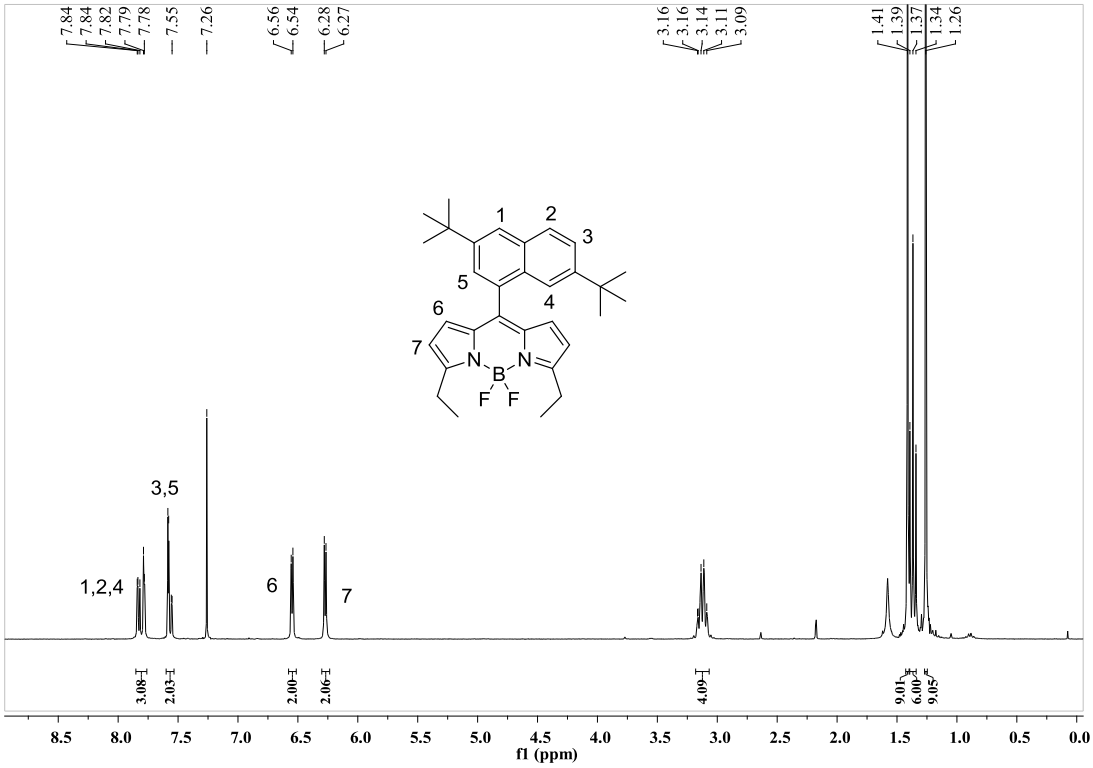

Fig. S9. ^{1}H NMR spectrum of compound **1** (300MHz, $CDCl_3$).

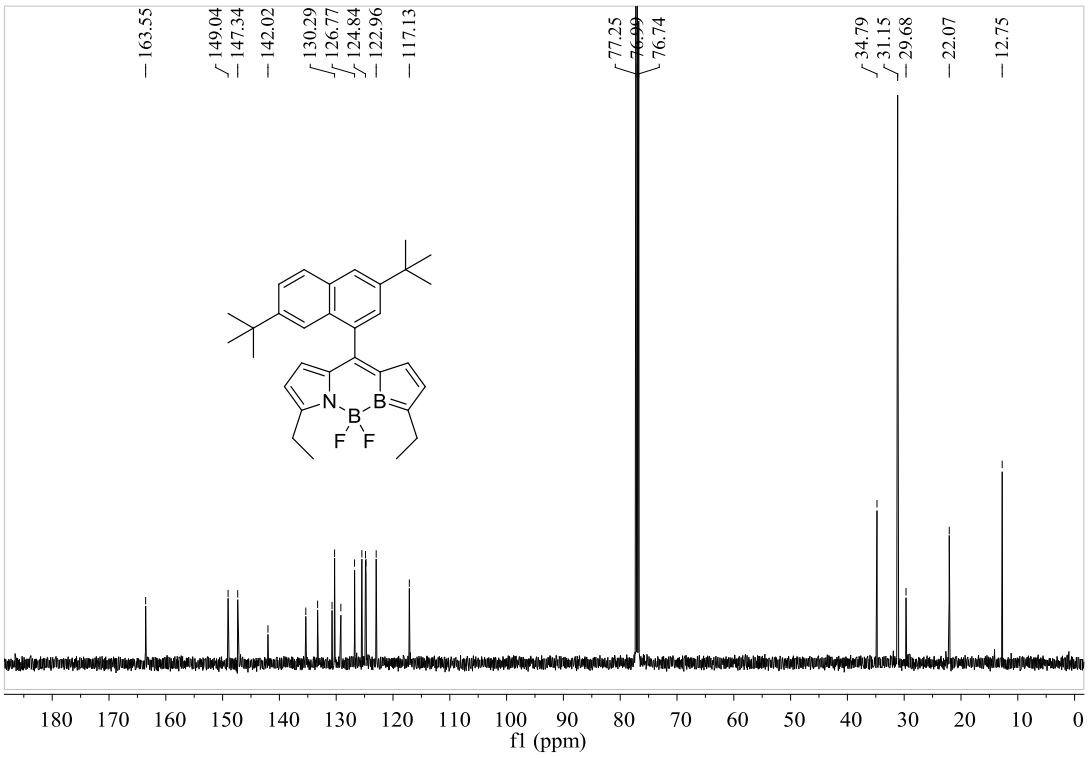

Fig. S10. ^{13}C NMR spectrum of compound **1** (126MHz, $CDCl_3$).

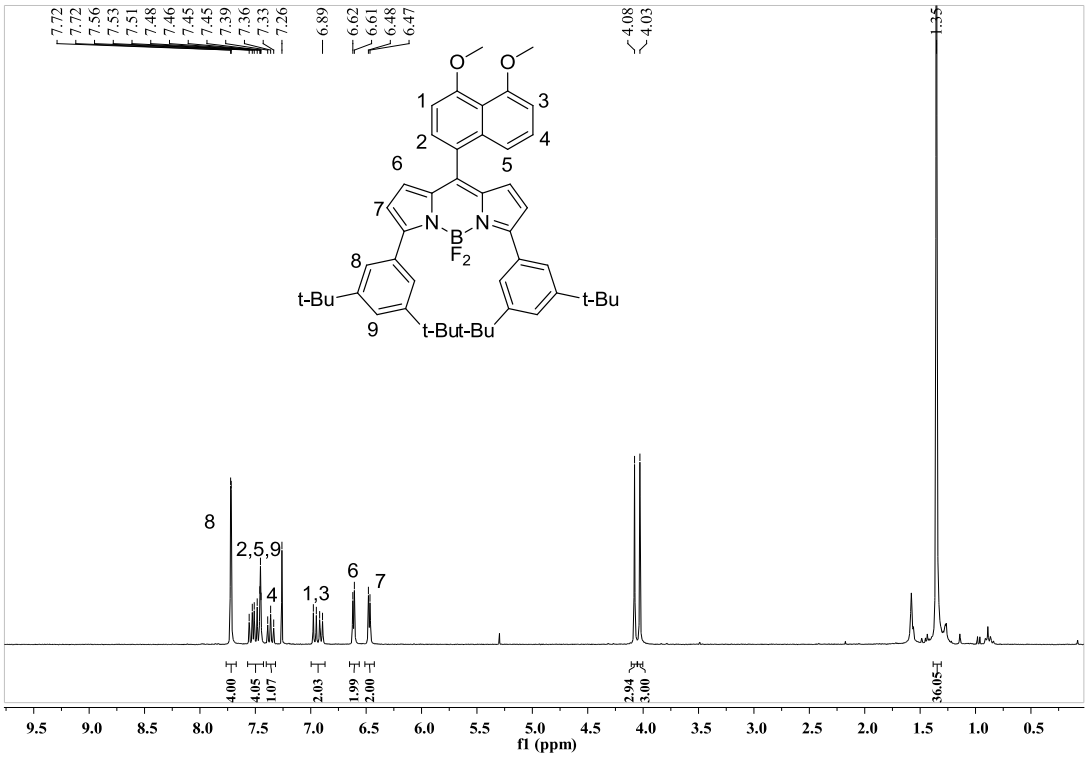

Fig. S11. ^{1}H NMR spectrum of compound **2** (300MHz, $CDCl_3$).

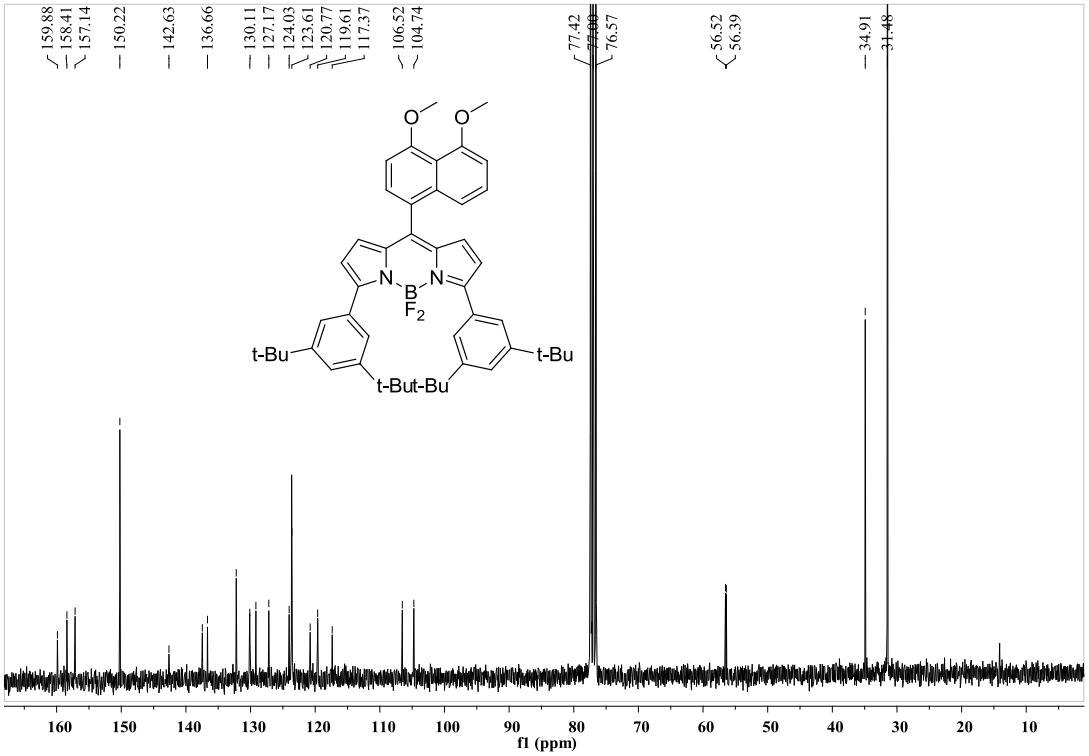

Fig. S12. ^{13}C-NMR spectrum of compound **2** (75MHz, $CDCl_3$).

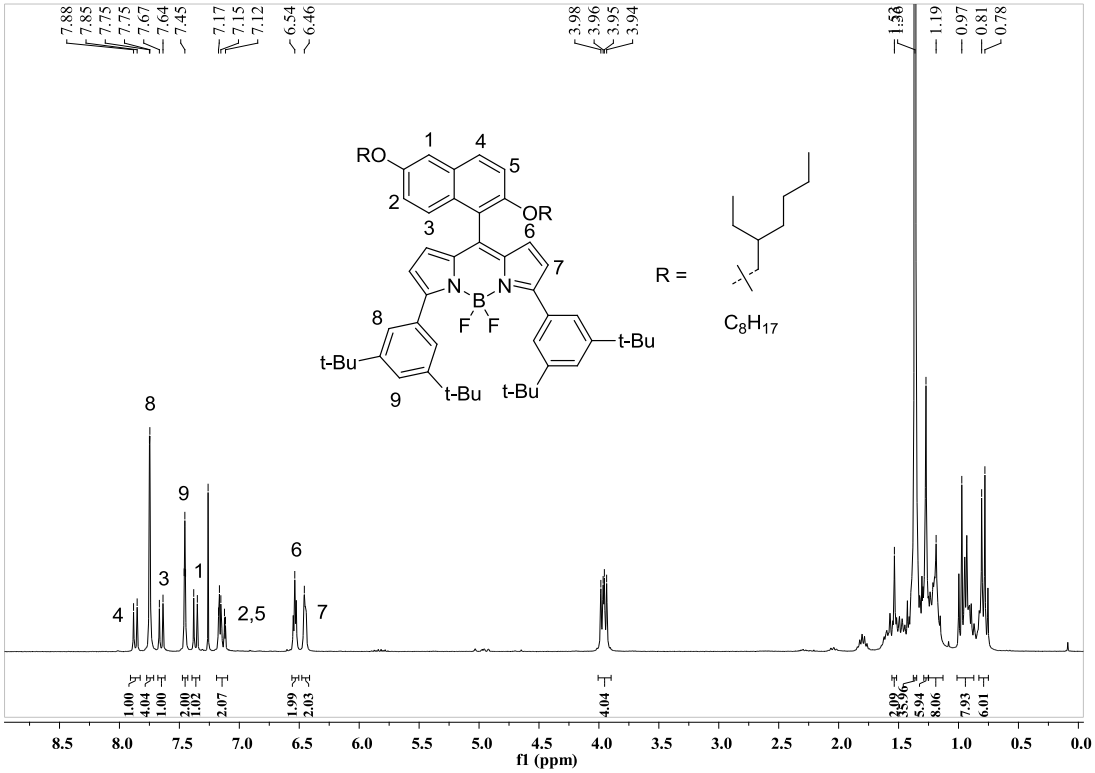

Fig. S13. ^{1}H-NMR spectrum of compound **3** (300MHz, $CDCl_3$).

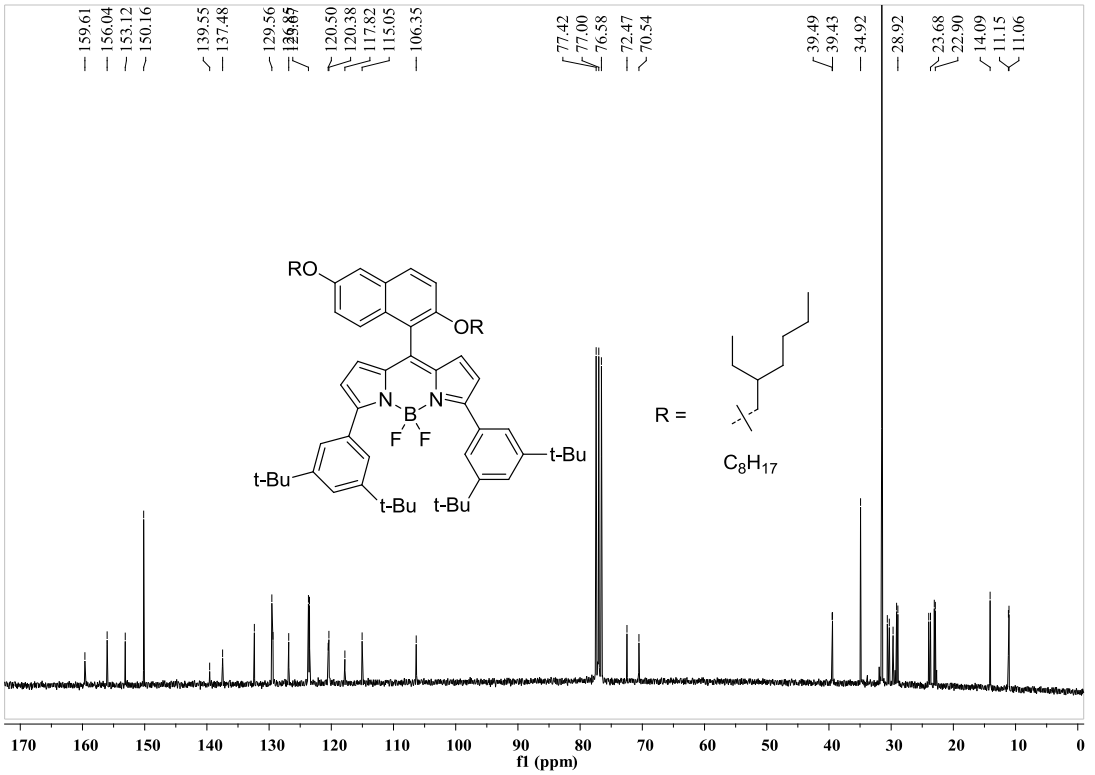

Fig. S14. ^{13}C NMR spectrum of compound **3** (75MHz, $CDCl_3$).

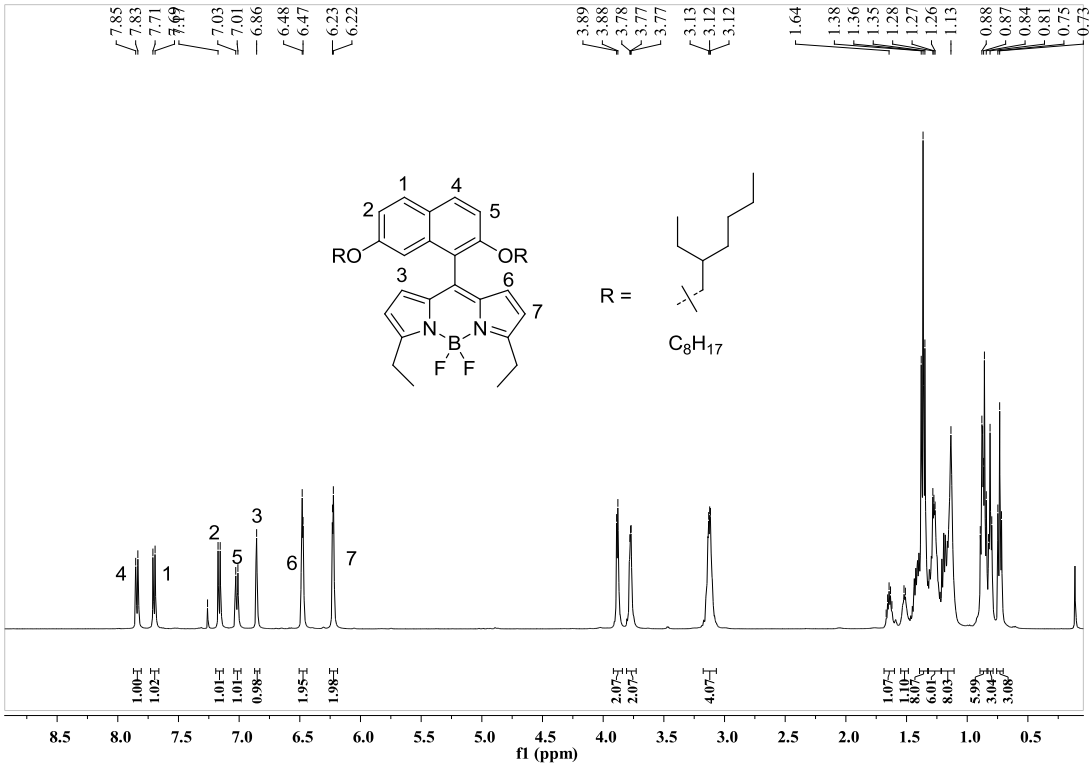

Fig. S15. ^{1}H NMR spectrum of compound **4** (500MHz, $CDCl_3$).

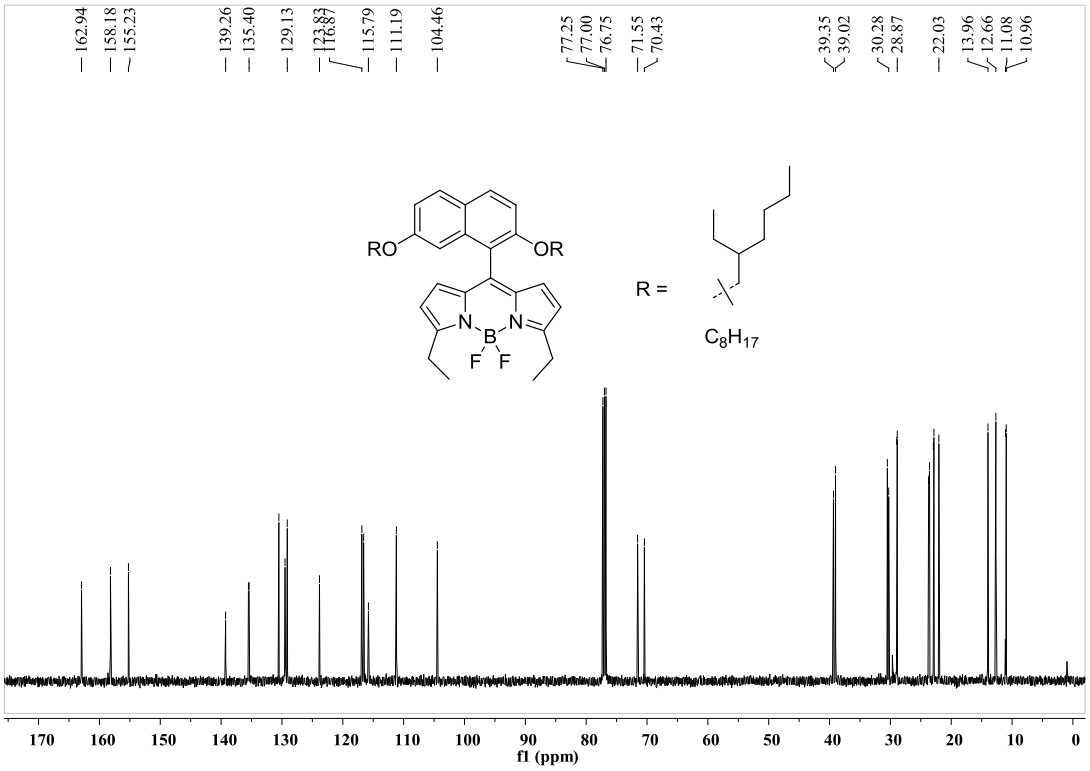

Fig. S16. ^{13}C NMR spectrum of compound **4** (126MHz, $CDCl_3$).

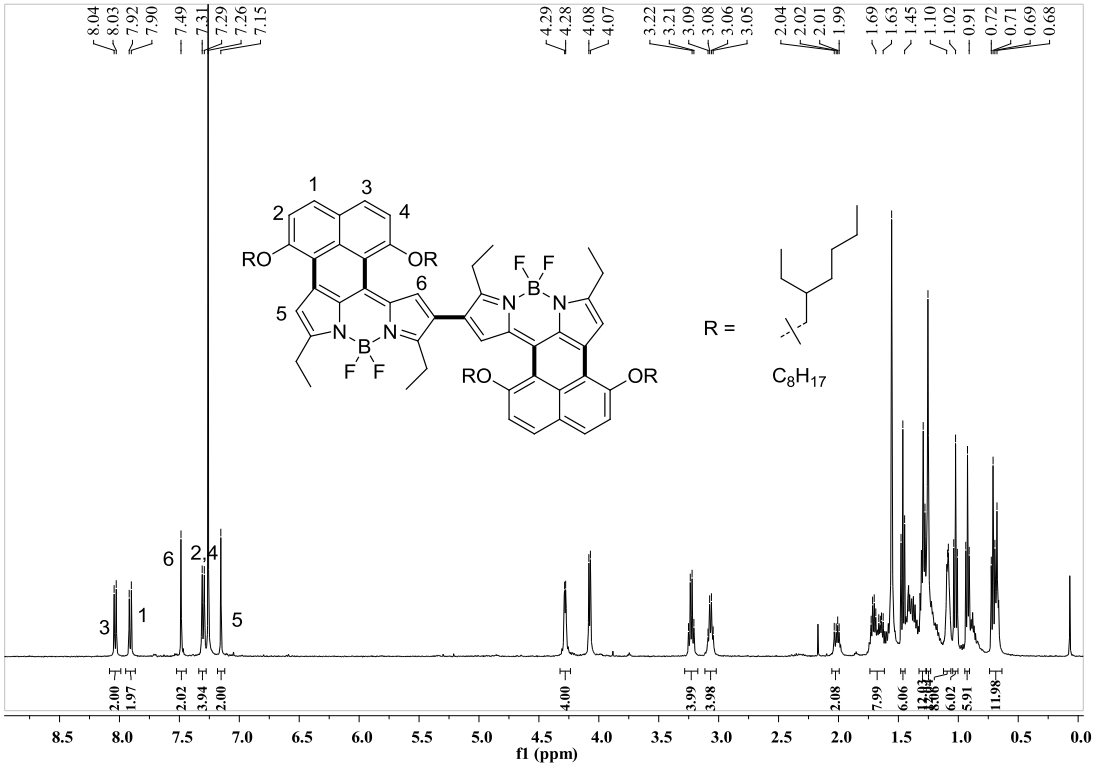

Fig. S17. ^{1}H NMR spectrum of compound **Na-BD** (500MHz, $CDCl_3$).

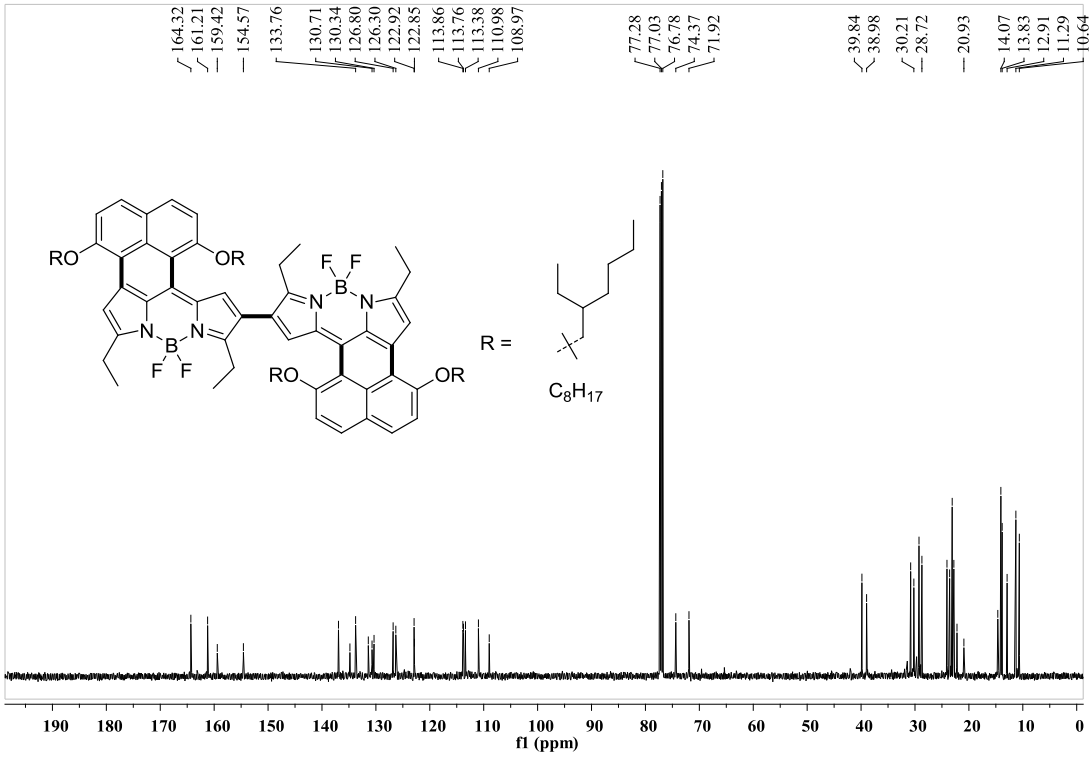

Fig. S18. ^{13}C NMR spectrum of compound **Na-BD** (126MHz, $CDCl_3$).

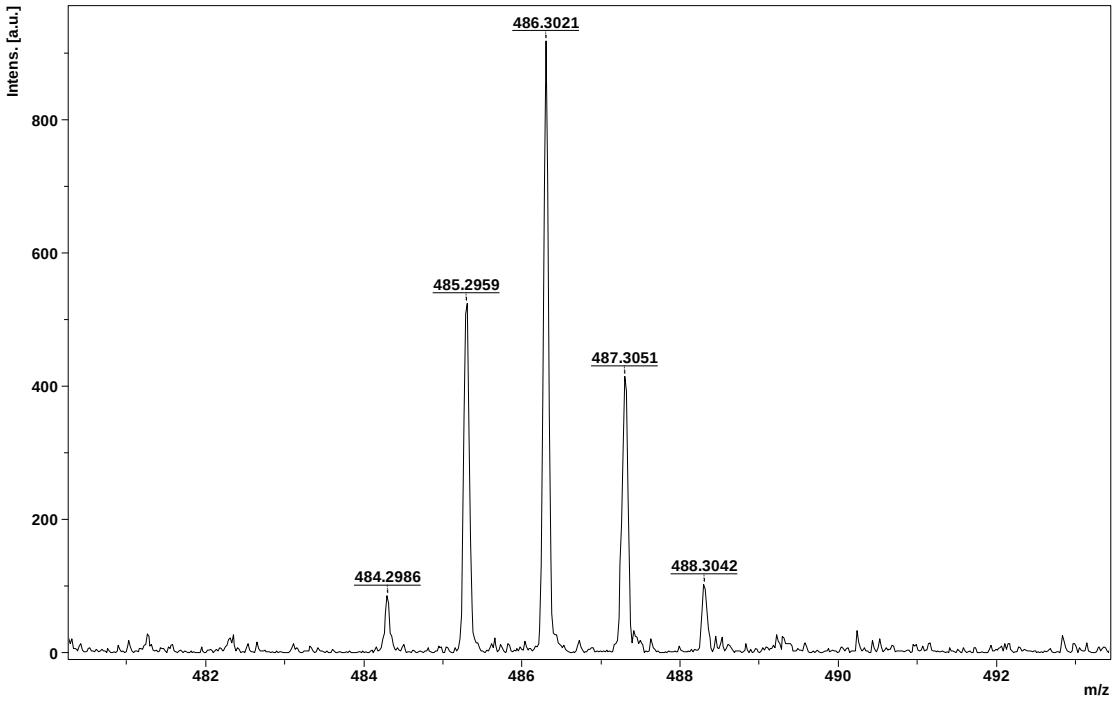

Fig. S19. HR mass spectrum (MALDI-TOF) spectrum of compound **1**.

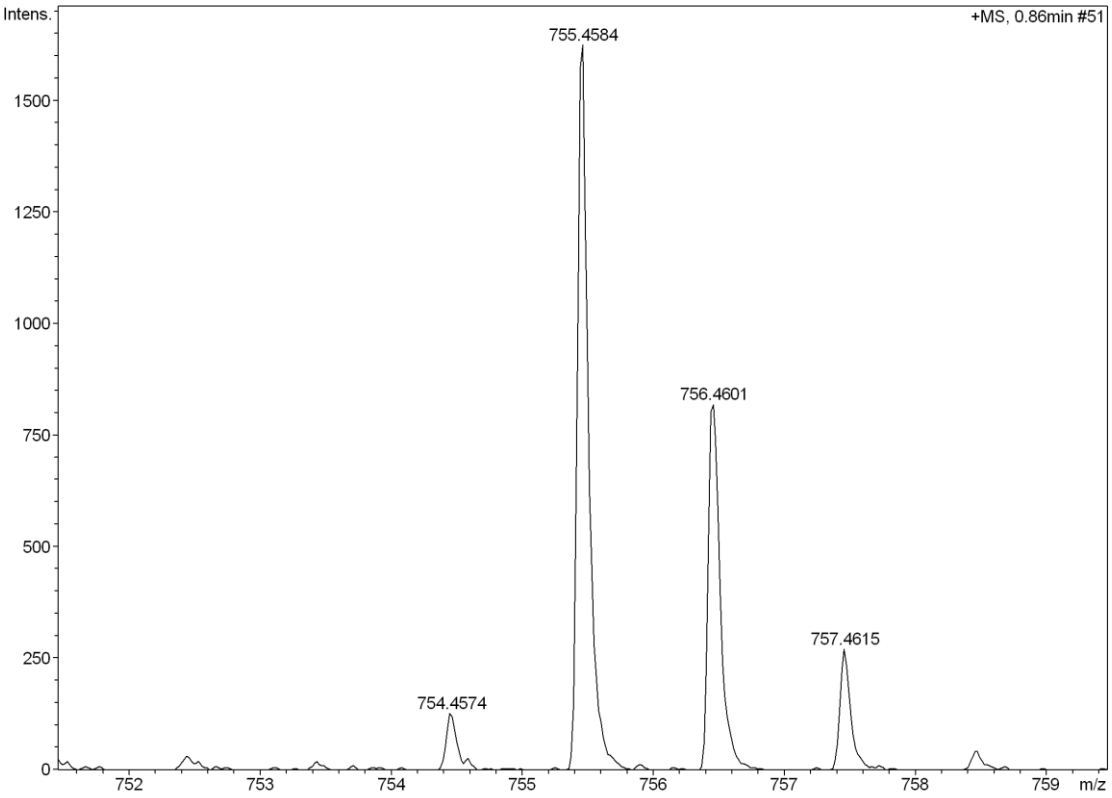

Fig. S20. HR mass spectrum (APCI) spectrum of compound **2**.

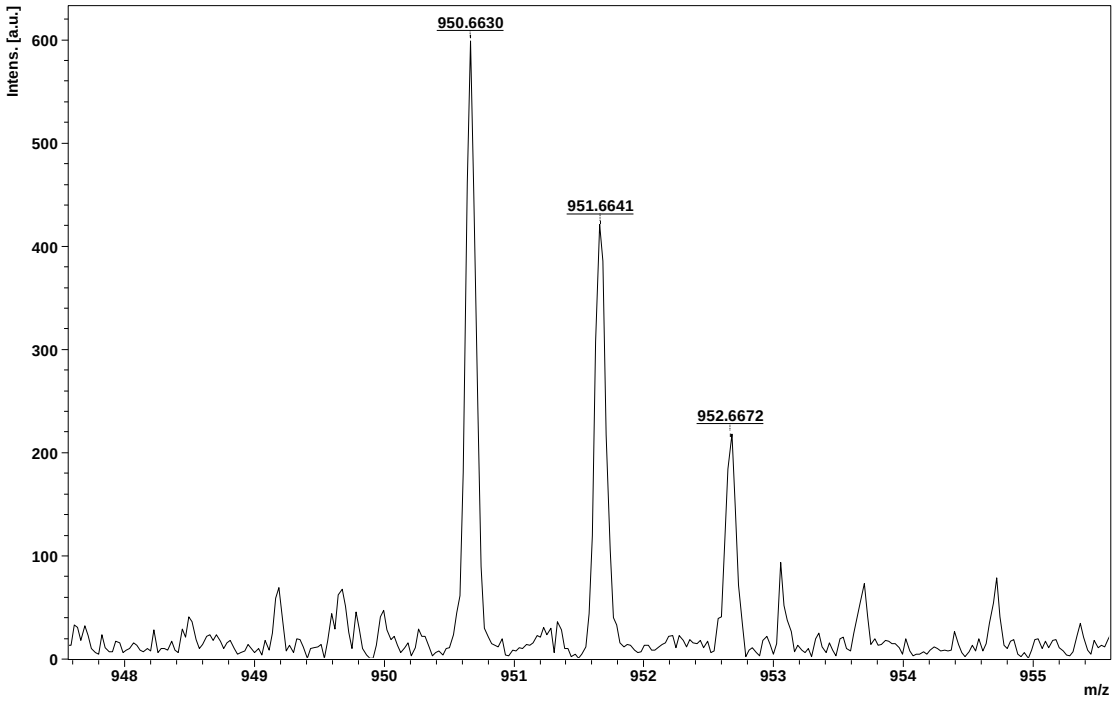

Fig. S21. HR mass spectrum (MALDI-TOF) spectrum of compound **3**.

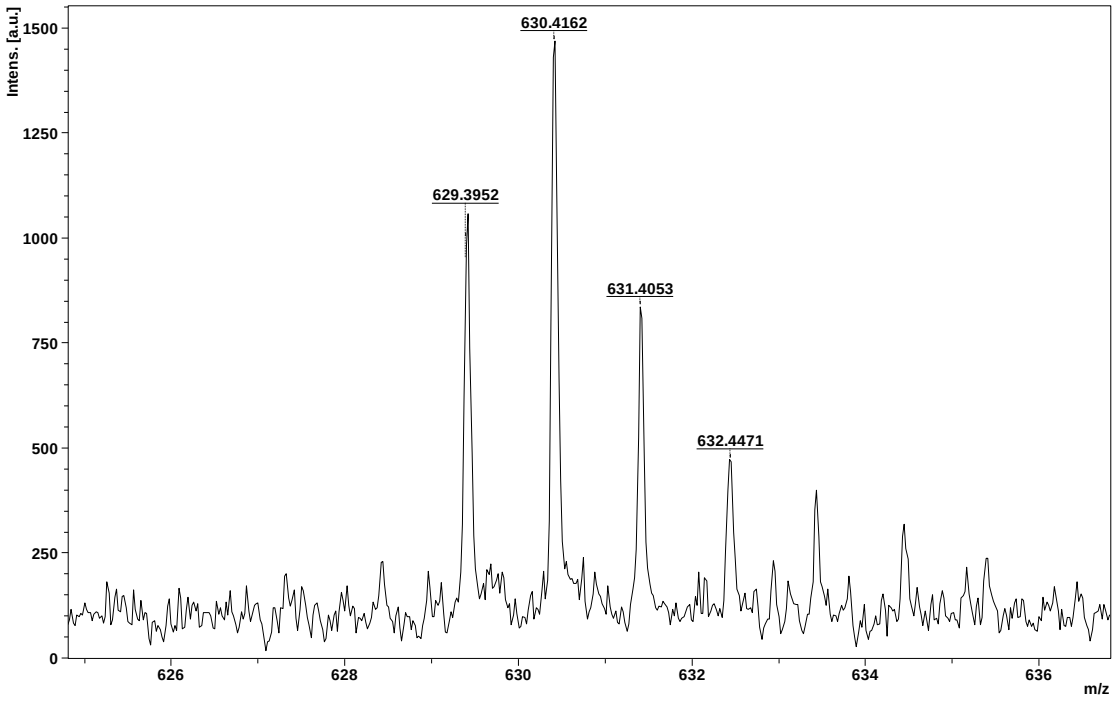

Fig. S22. HR mass spectrum (MALDI-TOF) spectrum of compound **4**.

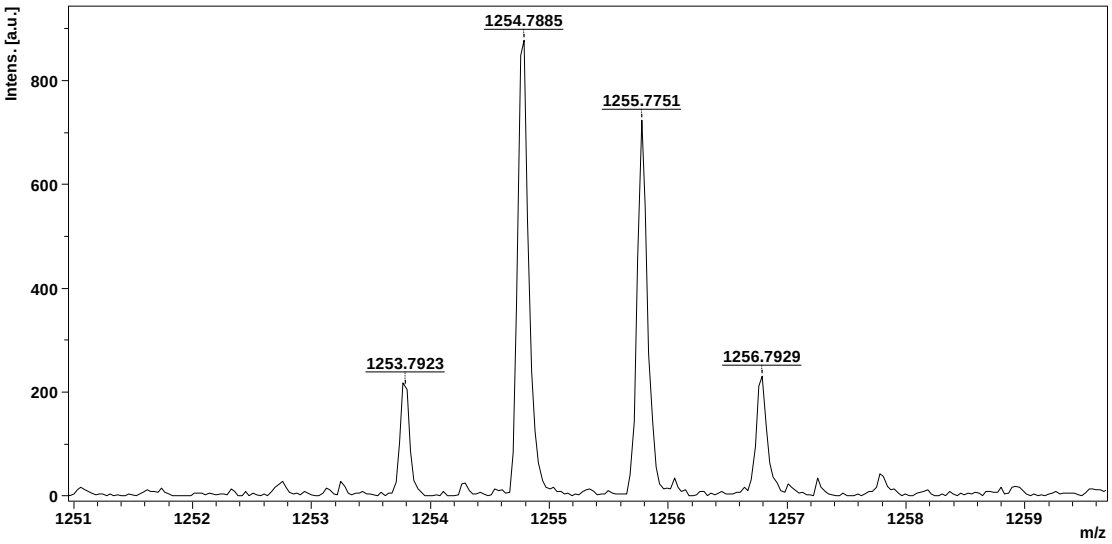

Fig. S23. HR mass spectrum (MALDI-TOF) spectrum of compound **Na-BD**.